

Supporting Information

Hierarchical Self-Assembly of Alkynylplatinum(II) Bzimy-Functionalized Metallacage via Pt··Pt and π - π Interactions

Ying Zhang,^{†,§} Qi-Feng Zhou,^{‡,§} Gui-Fei Huo,[‡] Guang-Qiang Yin,[‡] Xiao-Li Zhao,[‡] Bo Jiang^{*,‡}, Hongwei Tan^{*,†}, Xiaopeng Li,[†] Hai-Bo Yang^{*,‡}

[†]Department of Chemistry, Beijing Normal University, Beijing 100050, P. R. China

[‡]Shanghai Key Laboratory of Green Chemistry and Chemical Processes, School of Chemistry and Molecular Engineering, East China Normal University, Shanghai 200062, P. R. China

[†]Department of Chemistry, University of South Florida, Tampa, Florida 33620, United States

Table of Contents

1. Materials and methods.....	S2
2. Experimental details for synthesis and characterization of new compounds.....	S3
3. UV-vis absorption spectra and emission spectra.....	S5
4. Stimuli-responsive behavior of cage 2	S7
5. SEM tests.....	S9
6. The copy of ¹ H, ¹⁹ F NMR, and MS spectra of new compounds.....	S9

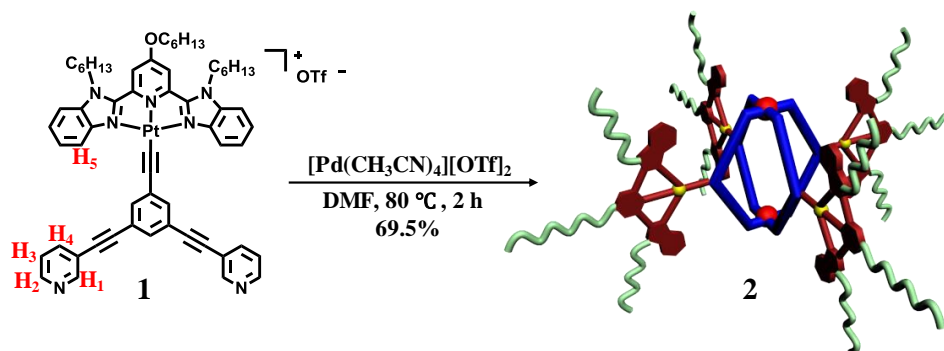
1. Materials and methods

All solvents were dried according to standard procedures and all of them were degassed under N₂ for 30 minutes before use. All air-sensitive reactions were carried out under inert N₂ atmosphere. ¹H and ¹⁹F NMR spectra were recorded on Bruker 500 MHz Spectrometer at 298 K. The ¹H chemical shifts are reported relative to the residual solvent signals. Coupling constants (*J*) are denoted in Hz and chemical shifts (*δ*) in ppm. Multiplicities are denoted as follows: s = singlet, d = doublet, m = multiplet, br = broad. The CSI-TOF-MS spectra were acquired by using an AccuTOF CS mass spectrometer (JMS-T100CS, JEOL, Tokyo, Japan). UV-vis spectra were recorded in a quartz cell (light path 10 mm or 2 mm) on a Cary 50Bio UV-visible spectrophotometer. Steady-state fluorescence spectra were recorded in a conventional quartz cell (light path 10 mm or 2 mm) on a Cary Eclipse fluorescence spectrophotometer. SEM images were obtained by using a S-4800 (Hitachi Ltd.) with an accelerating voltage of 3.0-10.0 kV. Samples were prepared by dropping dilute gels onto a silicon wafer. To minimize the charge of samples, a thin layer of Au was deposited onto the samples before SEM examination.

2. Experimental details for synthesis and characterization of new compounds

The ligand **1** was synthesized according to reported procedures.¹

Scheme S1. Self-assembly of functionalized metallacage **2**.



Self-assembly of functionalized metallacage 2. The dipyrindyl donor ligand **1** (26.67 mg, 21.73 μmol) and $[\text{Pd}(\text{CH}_3\text{CN})_4][\text{OTf}]_2$ (6.18 mg, 10.87 μmol) were weighed accurately into a glass vial. To the vial was added 0.5 mL DMF. The reaction solution was then stirred at 80 °C for 2 h to yield a homogeneous yellow solution. Then the diethyl ether was added into the bottle with continuous stirring (5 min) to precipitate the product. The reaction mixture was centrifuged, washed several times with DCM, and dried. The red product **2** (21.60 mg, 69.5%) was collected and re-dissolved in $\text{DMF-}d_7$ for NMR analysis. ^1H NMR (500 MHz; $\text{DMF-}d_7$): δ 9.93 (s, 8H), 9.73 (d, 8H, $J = 5.5$ Hz), 8.70 (d, 8H, $J = 8.2$ Hz), 8.49 (d, 8H, $J = 8.0$ Hz), 8.21 (d, 8H, $J = 8.4$ Hz), 8.13 (s, 8H), 7.93 (s, 8H), 7.71 (s, 4H), 7.67 (t, 8H), 7.62 (t, 8H), 5.16 (s, 16H), 4.68 (s, 8H), 2.12 (t, 16H), 1.95 (t, 8H), 1.28-1.55 (m, 72H), 0.93 (t, 12H), 0.85 (t, 24H). ESI-TOF-MS of **2**: calcd for $\text{C}_{240}\text{H}_{244}\text{F}_{12}\text{N}_{28}\text{O}_{16}\text{Pd}_2\text{Pt}_4\text{S}_4$ $[\text{M} - 4\text{OTf}]^{4+}$: 1280.6067, found: 1280.6482; calcd for $\text{C}_{239}\text{H}_{244}\text{F}_9\text{N}_{28}\text{O}_{13}\text{Pd}_2\text{Pt}_4\text{S}_3$ $[\text{M} - 5\text{OTf}]^{5+}$: 994.4918, found: 994.4092; calcd for $\text{C}_{238}\text{H}_{244}\text{F}_6\text{N}_{28}\text{O}_{10}\text{Pd}_2\text{Pt}_4\text{S}_2$ $[\text{M} - 6\text{OTf}]^{6+}$: 803.9218, found: 803.9813; calcd for $\text{C}_{237}\text{H}_{244}\text{F}_3\text{N}_{28}\text{O}_7\text{Pd}_2\text{Pt}_4\text{S}$ $[\text{M} - 7\text{OTf}]^{7+}$: 667.7956, found: 667.6943; calcd for $\text{C}_{236}\text{H}_{244}\text{N}_{28}\text{O}_4\text{Pd}_2\text{Pt}_4$ $[\text{M} - 8\text{OTf}]^{8+}$: 565.7014, found: 565.6115.

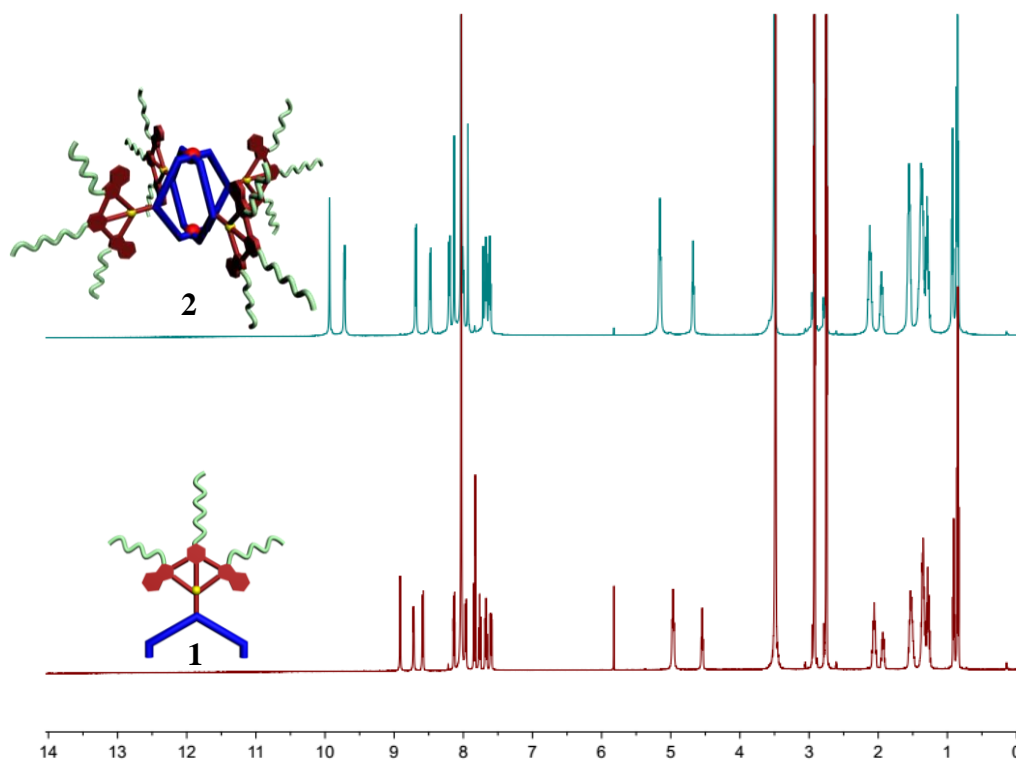


Figure S1. ^1H NMR spectra (500 MHz, in $\text{DMF-}d_7$, 298 K) of donor **1** and its corresponding self-assembled metallacycle **2**.

Reference:

(1) Jiang, B.; Zhang, J.; Ma, J.-Q.; Zheng, W.; Chen, L.-j.; Sun, B.; Li, C.; Hu, B.-W.; Tan, H.; Li, X.; Yang, H.-B. Vapochromic Behavior of a Chair-Shaped Supramolecular Metallacycle with Ultra-Stability. *J. Am. Chem. Soc.* **2016**, *138*, 738-741.

3. UV-Vis absorption spectra and emission spectra

UV-vis absorption and emission spectra of the ligand **1** was also studied in the mixed solvents of DMF and H₂O. As shown in Figure S2, with the increasing of water content, the absorption bands at around 300 nm and 350 nm gradually dropped in intensity accompanied by the growth of absorption tails beyond 450 nm in the UV-vis absorption spectra of **1**, indicating the existence of intermolecular Pt²⁺Pt and π - π stacking interactions. In the corresponding emission spectroscopy, a significant enhancement in emission intensity at $\lambda = 616$ nm was observed when the ration of water was 60%, suggesting that the ligand **1** also shown the solvent-induced emission switch in the mixed solvents of H₂O and DMF. All the above results indicated that the complex **2** retained the optical properties of ligand **1** rather than a significant quenching of the ligand's fluorescence by the Pd²⁺ ions after the formation of self-assembled cage. Notably, although the ligand **1** have similar optical properties to the complex **2** in the mixed solvents of H₂O and DMF, the well-defined cavity and the stimuli-responsive behavior of cage **2** endowed it with potential application in controllable encapsulation and release through host-guest interactions, which could not be achieved by the ligand **1**.

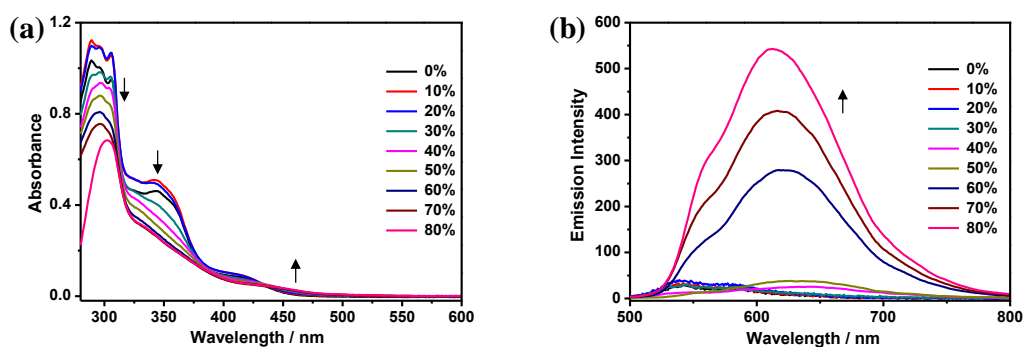


Figure S2. (a) UV-vis absorption and (b) emission spectra of ligand **1** (1.0×10^{-5} M) in DMF with increasing water content at 298 K.

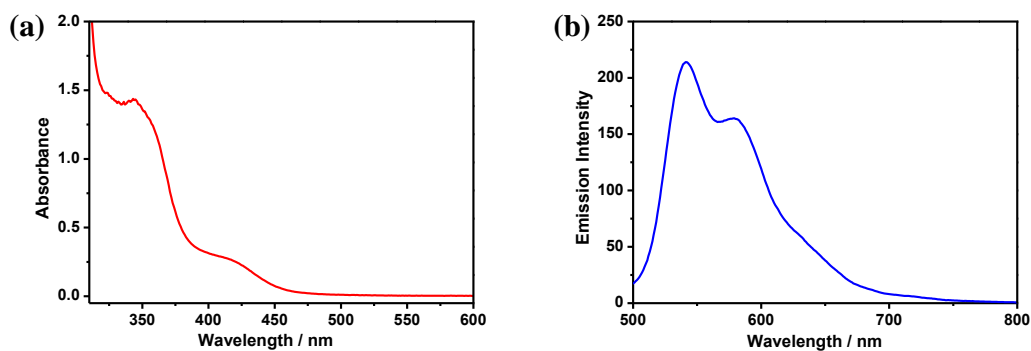


Figure S3. (a) UV-vis absorption and (b) emission spectra of metallage **2** (1.0×10^{-5} M) in DMF at 298 K.

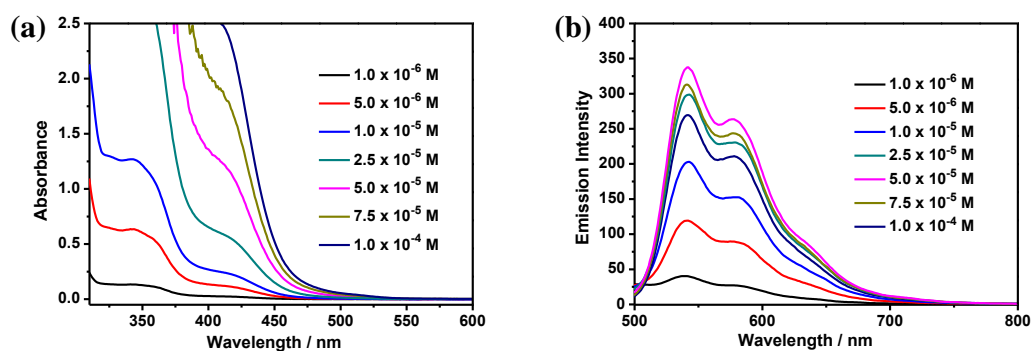


Figure S4. Concentration-dependent (a) UV-vis absorption and (b) emission spectra of metallage **2** in DMF at 298 K.

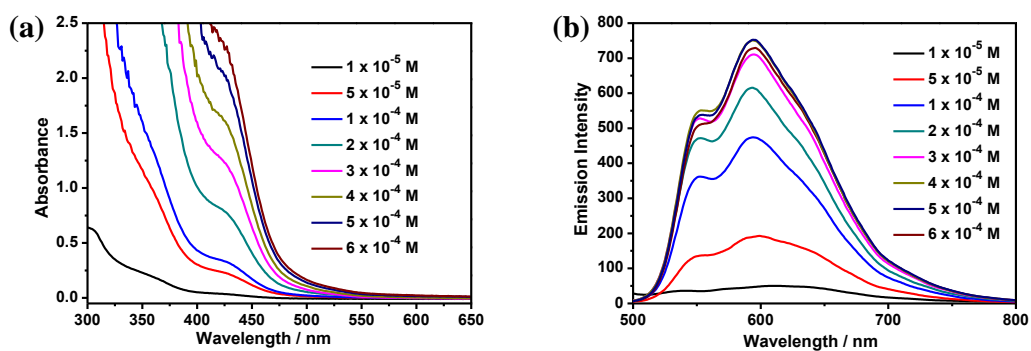


Figure S5. Concentration-dependent (a) UV-vis absorption and (b) emission spectra of metallage **2** in DMF/H₂O ($v/v = 1/1$) at 298 K.

4. Stimuli-responsive behavior of cage 2

Interestingly, the metallogel **2** shown stimuli-responsive behavior. As shown in Figure S6, when $(n\text{-C}_4\text{H}_9)_4\text{NCl}$ (16.0 equiv) was added to the surface of metallogel **2**, the metallogel was gradual collapse. In view of the existence of well-defined cavity and the stimuli-responsive behavior, the cage **2** have potential application in controllable encapsulation and release through host-guest interactions, which could not be achieved by the ligand **1**.

To understand the driving forces for the collapse of the metallogel **2** induced by $(n\text{-C}_4\text{H}_9)_4\text{NCl}$, ^1H NMR spectroscopy studies were performed. As shown in Figure S7, after the addition of $(n\text{-C}_4\text{H}_9)_4\text{NCl}$ (4.0 equiv) to the solution of **2** (1.3 mM) in $\text{DMF-}d_7$, proton signals assigned to free ligand **1** were found, suggesting that chloride ions were displacing some of the ligands **1** from the cage **2**. Furthermore, when over 8.0 equivalents of $(n\text{-C}_4\text{H}_9)_4\text{NCl}$ was added, typical proton signals of cage **2** disappeared, which indicated the complete disassembly of cage **2**. Such NMR spectroscopy experiments provided direct evidence for the halide-induced disassembly of cage **2**. Thus, the metallogel **2** was collapse when the $(n\text{-C}_4\text{H}_9)_4\text{NCl}$ was added.

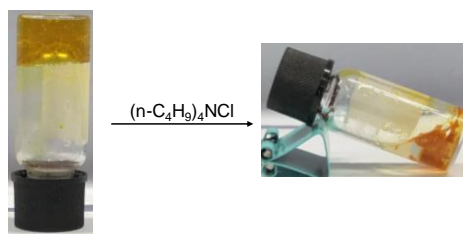


Figure S6. Photographs of metallogel **2** before and after the addition of $(n\text{-C}_4\text{H}_9)_4\text{NCl}$.

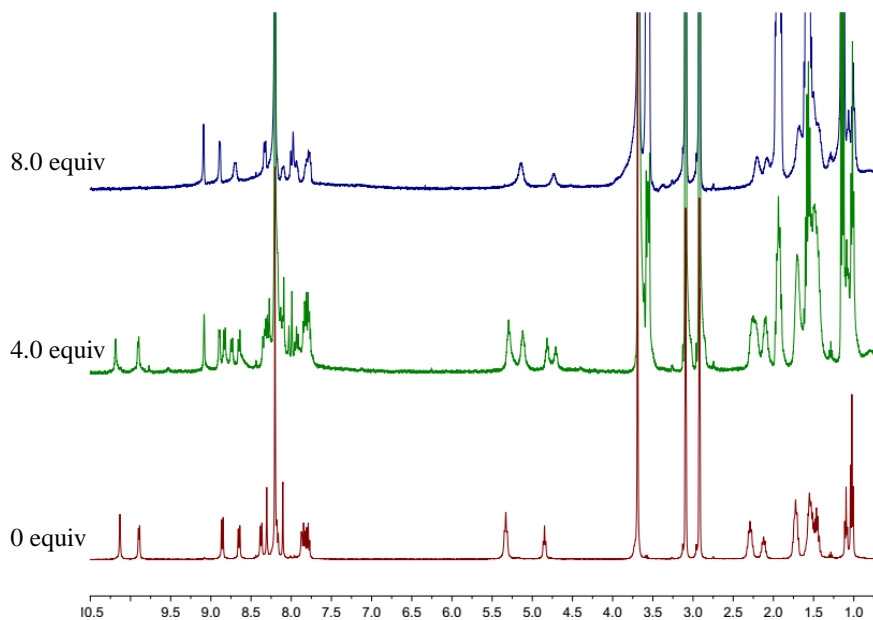


Figure S7. ^1H NMR spectra of cage **2** ($[\mathbf{2}] = 1.3 \times 10^{-3}$ mol/L) in $\text{DMF-}d_7$ with the addition of $(n\text{-C}_4\text{H}_9)_4\text{NCl}$.

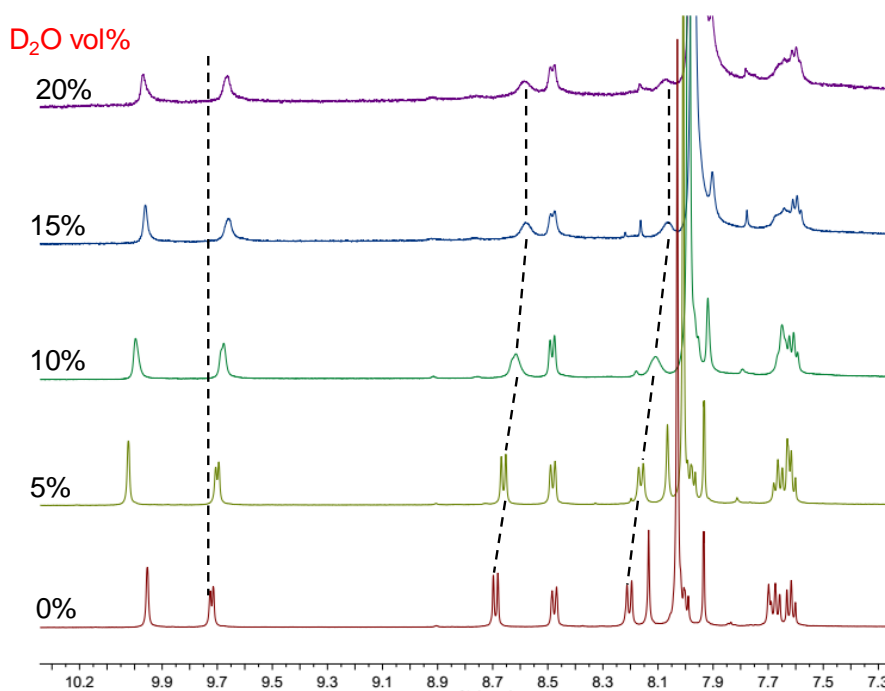


Figure S8. Partial ^1H NMR spectra (500 MHz) of **2** ($[\mathbf{2}] = 1.3 \times 10^{-3}$ M) in $\text{DMF-}d_7$ with increasing D_2O content at 298 K.

5. SEM tests

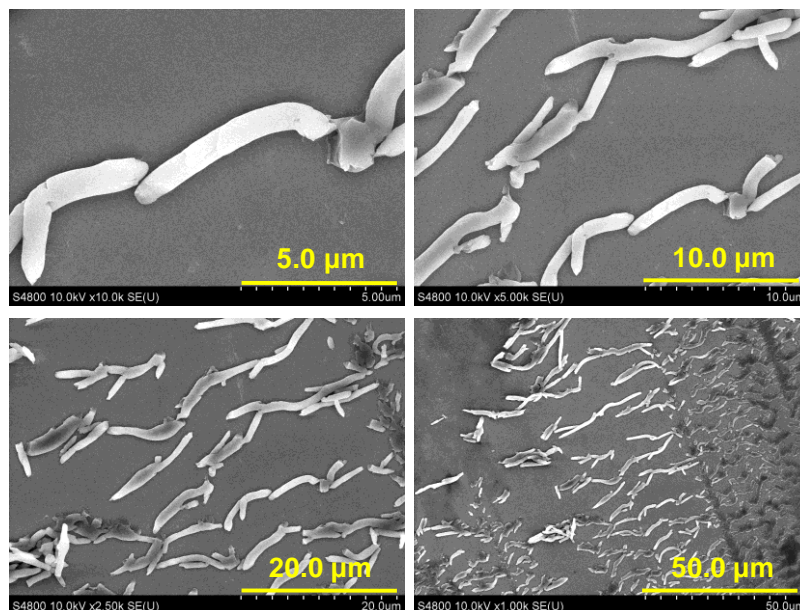
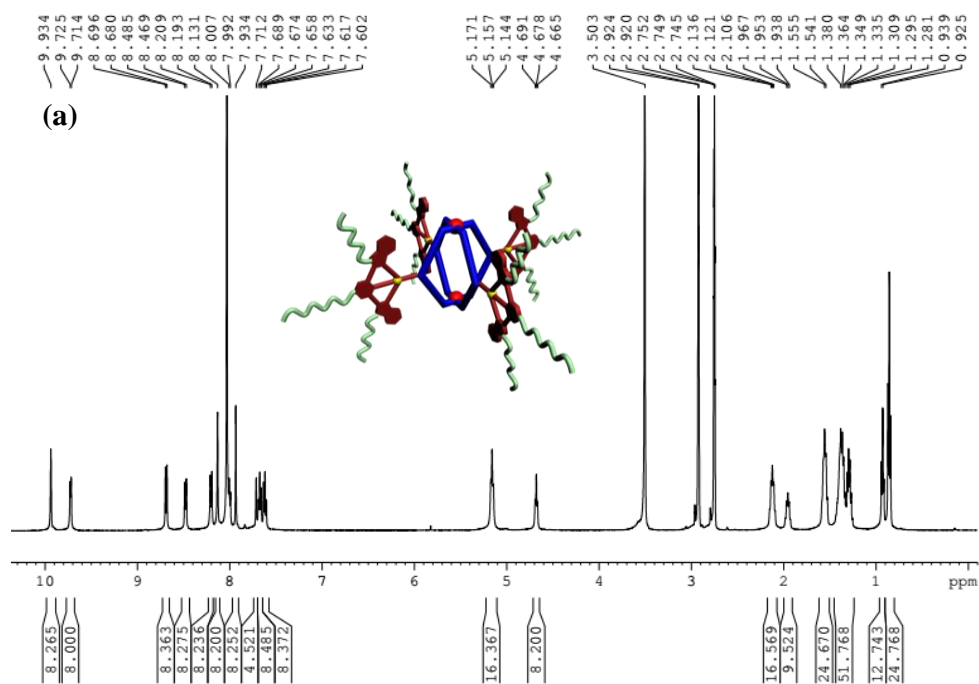


Figure S9. SEM images of the xerogel of 2 in DMF/H₂O = 1:1.

6. The copy of ¹H, ¹⁹F NMR, and MS spectra of new compounds



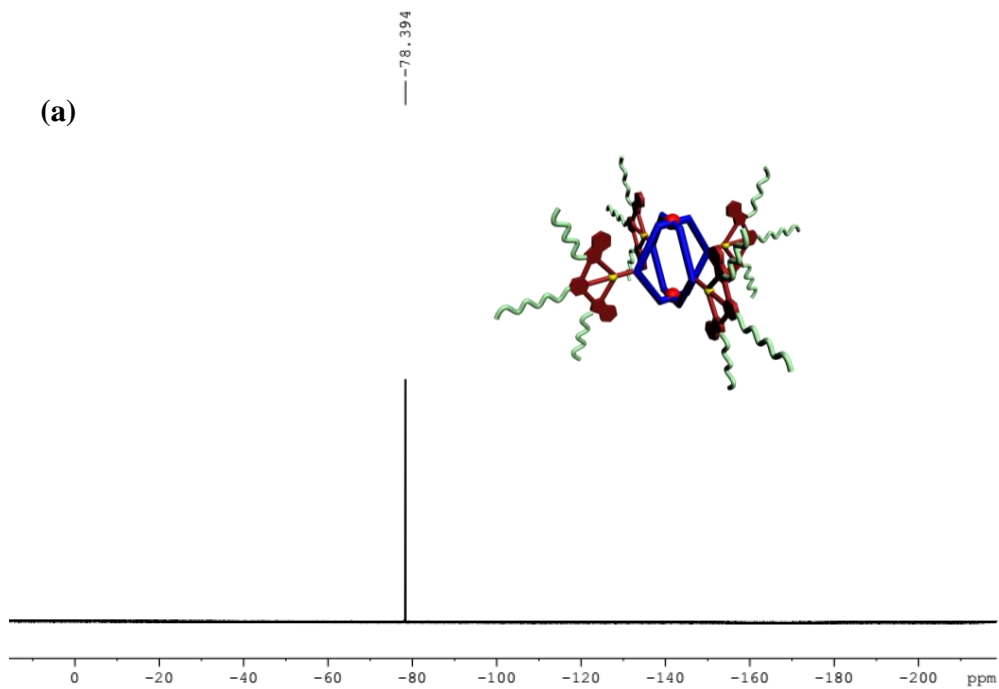


Figure S10. (a) ^1H NMR spectrum (500 MHz, $\text{DMF-}d_7$, 298 K) and (b) ^{19}F NMR spectrum (300 MHz, $\text{DMF-}d_7$, 298 K) of metallacage **2**.

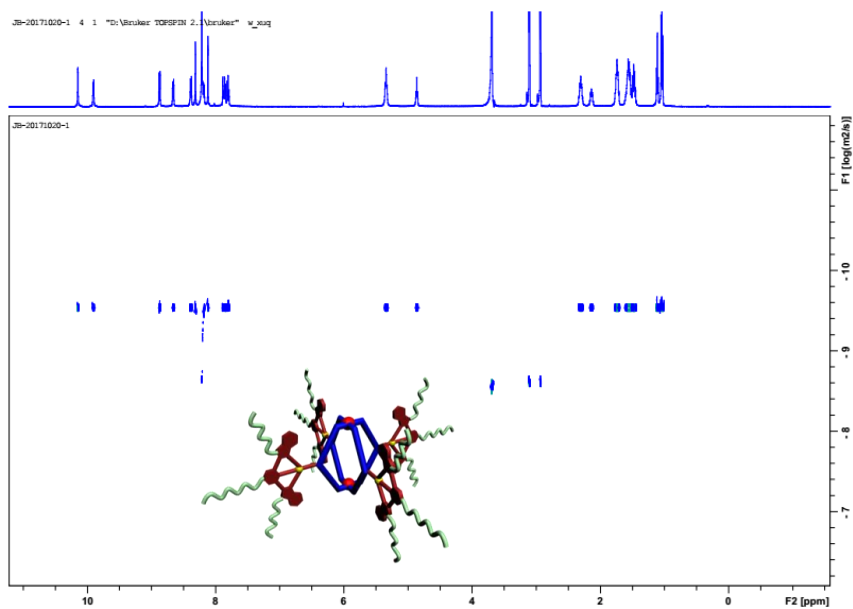


Figure S11. DOSY NMR spectrum (500 MHz, $\text{DMF-}d_7$, 298 K) of metallacage **2**.

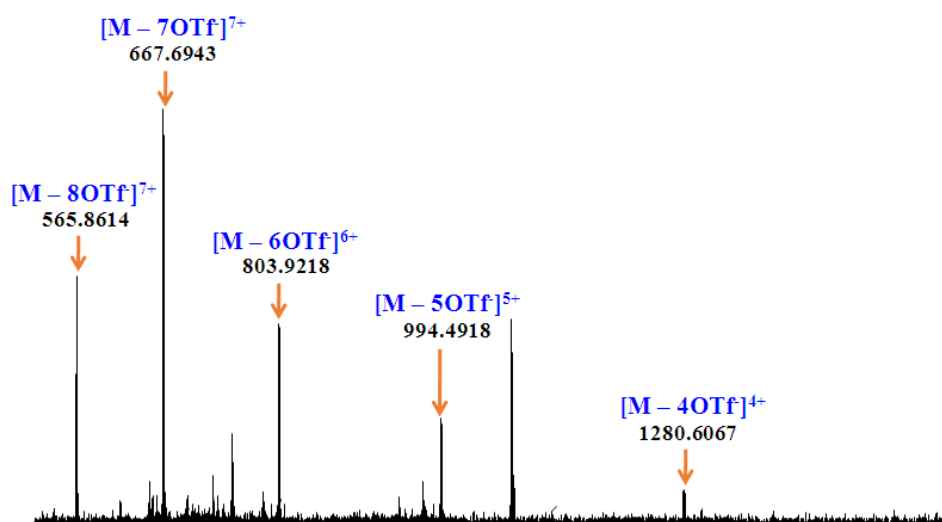


Figure S12. ESI-TOF-MS spectrum of metallacage 2.